A PRESSURE EVOLUTION EQUATION FOR THE PARTICULATE PHASE IN INHOMOGENEOUS COMPRESSIBLE DISPERSE MULTIPHASE FLOWS

Subramanian Annamalai,[1, *] S. Balachandar,[1] P. Sridharan,[1] and T. L. Jackson[1]

[1]*Department of Mechanical and Aerospace Engineering,*
University of Florida Gainesville FL 32611.

1

Abstract

An analytical expression describing the unsteady pressure evolution of the dispersed phase driven by variations in the carrier phase is presented. In this article, the term 'dispersed phase represents rigid particles, droplets or bubbles. Letting both the dispersed and continuous phases to be inhomogeneous, unsteady and compressible, the developed pressure equation describes the particle response and its eventual equilibration with that of the carrier fluid. The study involves impingement of a plane traveling wave of a given frequency and subsequent volume-averaged particle pressure calculation due to a single wave. The ambient/continuous fluid's pressure and density-weighted normal velocity are identified as the source terms governing the particle pressure. Analogous to generalized Faxén's theorem which is applicable to particle equation of motion, the pressure expression is also written in terms of the surface average of time-varying incoming flow properties. The surface average allows the current formulation to be generalized for any complex incident flow, including situations where the particle size is comparable to that of the incoming flow. Further the particle pressure is also found to depend on the dispersed-to-continuous fluid density ratio and speed of sound ratio in addition to dynamic viscosities of both fluids. The model is applied to predict the unsteady pressure variation inside an aluminum particle subjected to normal shock waves. The results are compared against numerical simulations and found to be in good agreement. Furthermore, it is shown that although the analysis is conducted in the limit of negligible flow Reynolds and Mach numbers, it can be used to compute the density and volume of the dispersed phase to reasonable accuracy. Finally, analogous to the pressure evolution expression, an equation describing the time-dependent particle radius is deduced and is shown to reduce to the Rayleigh-Plesset equation in the linear limit.

---
* subbu.ase@ufl.edu

I. INTRODUCTION

Dispersed multiphase flows (as opposed to separated multiphase flows) concerns fluid systems where there exists discrete particles in an otherwise continuous fluid media. It is important to note that, throughout this study, by 'dispersed' or 'particulate' phase we mean air bubbles, liquid droplets or rigid solid particles such as sand, alumina or dust particles, situated in a surrounding fluid, termed the 'carrier' or 'continuous' phase [1]. A dispersed multiphase flow greatly simplifies when the dispersed phase (particles) is in perfect equilibrium with the surrounding continuous phase. In other words, in the limit where the dispersed phase pressure, velocity and temperature are instantaneously equal to the corresponding pressure, velocity and temperature of the local surrounding continuous phase, the multiphase system can be studied as a mixture, without needing to separately account for the time evolution of the mass, momentum and energy of the individual phases. In this limit, it is sufficient to solve the governing equations of the mixture (or the carrier phase accounting for the volume fraction of the different phases) and the particles are transported along with the fluid and this limit is often called the dusty gas approach [2, 3]. However this approach is limited to particles of negligible inertia, since perfect pressure, velocity and temperature equilibrium between the phases is assumed, and such perfect equilibrium is not satisfied in most multiphase applications.

In situations where the inertia of the dispersed phase (particles) is not negligible, there will be disequilibrium between the two phases. We identify three primary equilibrium processes between the dispersed and the continuous phases; these are equilibrium of pressure, velocity and temperature. For example, if the continuous phase pressure suddenly changes within a reference volume of fluid at the macroscale, the particles dispersed within this reference volume will respond by evolving towards this new pressure with an appropriate change in density and specific volume, as dictated by the equation of state. Similarly, if the continuous phase velocity or temperature suddenly changes within a reference volume, the velocity or temperature of the particles within that volume will evolve towards their new values, due to momentum and energy exchange between the continuous and the dispersed phases.

Starting from the pioneering work of Stokes [4] the velocity equilibrium process has been well studied. In the quasi-steady limit, where the unsteady effects can be ignored, the relative velocity between the dispersed/particulate and the continuous phases leads to the

simplest particle equation of motion:

$$\frac{\mathrm{d}\mathbf{u}^d}{\mathrm{d}t} = \frac{\mathbf{u}^c - \mathbf{u}^d}{\tau_{pV}}, \qquad \tau_{pV} = \frac{(2\tilde{\rho}+1)R^2}{9\nu^c\Phi_V}, \tag{1}$$

where $\mathbf{u}^d$ denotes the particle velocity and $\mathbf{u}^c$ denotes the fluid velocity at the particle location, t denotes time. In the definition of particle velocity time scale $\tilde{\rho}$, R, ν^c, and Φ_V are the particle-to-fluid density ratio, particle radius, kinematic viscosity of the fluid, and nonlinear correction to Stokes drag respectively. The equation of motion describes the approach to "velocity equilibrium" (or linear momentum equilibrium) where τ_{pV} denotes the time scale on which the dispersed phase approaches the continuous phase velocity, $\mathbf{u}^c$. If the time scale on which the continuous phase velocity changes is τ_{cV}, then a Stokes number can be defined as the time scale ratio: $St_V = \tau_{pV}/\tau_{cV}$. Only in the limit $St_V \ll 1$ the dispersed phase (particles) can be taken to be in near-perfect equilibrium with the continuous phase (i.e., $\mathbf{u}^d \approx \mathbf{u}^c$). Otherwise, the dispersed phase is not in local instantaneous equilibrium with the continuous phase and the dispersed phase dynamics will be given by the equation of motion.

If unsteady effects, arising from the acceleration of the continuous or the dispersed phase, become important, then the dispersed phase (particle) velocity is governed by the more involved Basset-Boussinesq-Oseen (BBO) [5–7] equation of motion. Further improvements to the BBO equation exists and they rigorously include the effects of finite particle size, internal motion within the dispersed phase (rigid particles/bubbles/droplets), and compressibility [8–12]. Empirical extensions that account for the nonlinear effects of finite Reynolds and Mach numbers have also been advanced [13–16]. In essence, the approach to velocity equilibrium is well understood and expressed in terms of rigorous equations of motion in the linear limit and reliable empirical extensions in the nonlinear regime.

Analogous to velocity, the approach to "thermal equilibrium" arising from the temperature difference between the particle and the surrounding fluid is given by [17]:

$$\frac{\mathrm{d}T^d}{\mathrm{d}t} = \frac{T^c - T^d}{\tau_{pT}}, \qquad \tau_{pT} = \frac{\tilde{\rho}\, R^2 \widetilde{C_p}}{3\kappa^c\Phi_T}, \tag{2}$$

where, T^d represents the dispersed phase temperature while T^c denotes the temperature of the continuous medium. Here, τ_{pT} is the thermal response time of the particle. Analogous

to the velocity response time it denotes the time required for the dispersed phase to attain thermal equilibrium with the continuous phase. In Eq. (2), $\widetilde{C_p}$, κ^c and Φ_T denote the particle-to-fluid specific heat ratio, thermal diffusivity of the continuous phase and nonlinear correction to Nusselt number respectively.

While there are explicit equations governing the evolution of particle velocity and temperature (Eqs. (1), (2)), an equation that governs the dispersed phase pressure evolution (i.e., pressure interior of the particle) is lacking. In many dispersed multiphase flow applications in the incompressible regime, such as sediment transport, turbidity currents and fluidized bed reactors, the pressure of the dispersed phase is taken to be equal to that of the continuous phase, even when the dispersed phase (particle) velocity and temperature are taken to be different from those of the continuous phase, and the evolution of the dispersed phase velocity and temperature are given by equations of the form (1) and (2). The time scale of pressure equilibration is of the order of the acoustic time scale, which is given by $\tau_{pa} = R/a$, were a is the speed of sound, assuming the speed of sound within the dispersed and the continuous phases to be of the same order. In many applications the time scale ratios τ_{pa}/τ_{pV} and τ_{pa}/τ_{pT} are small and the assumption of pressure equilibrium is well justified. However, in applications such as bubbly flows, cavitation and propagation of an intense shock over a bed of particles, the assumption of pressure equilibrium between the dispersed and the continuous phases become inappropriate. In these situations, we require an equation for the evolution of the dispersed phase pressure, similar to those for dispersed phase velocity and temperature. Obtaining such an evolution equation for the dispersed phase pressure is the focus of the present work.

There is extensive literature [18–22] that investigates the behavior of isolated and dispersion of bubbles in liquids, where the evolution of pressure within the bubble plays an important role. In the study of bubbly flows, the rapid growth and collapse of air or vapor bubble is of significance since cavitation causes major damage to turbine blades and propellers. In such cases, the compressibility of the flow is important and one is interested in the time history of bubble radius and pressure [23, 24]. The growth rate of bubbles is governed by Rayleigh-Plesset equation [25, 26] and it has been observed both from theory and experiments [27–29] that their evolution is highly oscillatory. This non-monotonic behavior also translates to a non-monotonic evolution for the dispersed phase (bubble) pressure. Thus, there is an interesting difference between the process of pressure equilibration and the evo-

lution of dispersed phase velocity or temperature towards equilibrium. A sudden change in the continuous phase velocity or temperature leads to a monotonic change in the dispersed phase (particle) velocity or temperature, as represented by Eqs. (1) and (2). However a step change in the continuous phase pressure leads to a non-monotonic, oscillatory evolution of dispersed phase pressure along its path to equilibrium.

In applications involving shock-particle interaction, as the shock sweeps over the particle, the pressure within the particle is driven by a rapid change in the fluid pressure surrounding the particle. A micron-sized particle, initially at equilibrium with the pre-shock ambient condition, when subjected to an intense shock wave will undergo pressure change on the order of mega- to gigapascals in a few nanoseconds. In this scenario, the external post-shock pressure serves as the source term and drives the dispersed phase (rigid particles/bubbles/droplets) towards a new pressure equilibrium. The time scale of pressure variation within the particle is of the same order as the time scale on which the continuous phase pressure changes.

In Eq. (1), the right hand side is the point-particle model for the quasi-steady force exerted on a particle by the surrounding continuous phase, scaled by the mass of the particle. It is an approximation to the actual force on a particle, which could be calculated with a fully resolved simulation. But the advantage of the point-particle model is that it encapsulates the net effect of all the details of the flow around the particle at the microscale and expresses the quasi-steady force entirely in terms of the undisturbed continuous phase velocity at the macroscale. Point-particle force models such as the BBO equation and the Maxey-Riley-Gatignol (MRG) equation are systematic improvements upon Eq. (1). By taking into account additional effects such as unsteadiness and finite particle size, they provide better approximation to the net momentum exchange between the particle and the continuous phase flow. Similarly, Eq. (2) is a point-particle model for the net energy exchange between the particle and the continuous phase. However, to the best of our knowledge there appears to be no physical model/equation that dictates the pressure equilibration process.

The primary objective of the current work is to rigorously develop an equation for the time evolution of pressure of the dispersed phase (i.e., pressure inside the particle) purely in terms of the undisturbed macroscale flow properties of the continuous phase. We accomplish this by considering an arbitrary time-dependent spatially-varying ambient flow past a spherical particle and solving the linearized Navier-Stokes equations for both the inside and outside flows with appropriate matching at the interface. We allow both the dispersed

6

and continuous phases to be compressible and viscous. Therefore the pressure model to be developed in the present study can be regarded as analogue to the MRG equation for particle motion.

Towards this goal, in Sec. II, we begin by considering an acoustic wave of a given frequency and wavenumber to impinge on a stationary sphere. We solve the linearized compressible Navier-Stokes equations both inside and outside the sphere thus allowing for transmitted and scattered waves. The velocities are expressed as flow potentials (sum of infinite terms) and the monopole term alone dictates the volume-averaged pressure inside the particle. In this work we allow only for radial pulsations of the particle and no shape deformation is permitted. We impose no restriction on the particle size compared to the length scale of the incoming flow. Subsequently in Sec. III, the volume-averaged particle pressure is computed for a given wavenumber and frequency. Following our earlier work on generalized Faxén theorem [30], we establish (in Laplace space) the equivalence between volume-averaged pressure inside the particle (monopole term) corresponding to a single wavenumber/frequency and surface average of the incident pressure and velocity. The resulting expression is transformed to the time-domain (Laplace inverse) and the particle pressure is found to be a sum of two integral contributions arising from (i) undisturbed pressure and (ii) undisturbed radial velocity of the continuous phase. Furthermore each of the contributions is a convolution integral made up a temporal part, termed the kernel and a spatial part arising from the surface average of the undisturbed fluid quantity of the continuous phase. The behavior of the kernels for various combinations of continuous and dispersed phase media is analyzed. These kernels are found to be oscillatory, leading to the non-monotonic behavior seen in the particle pressure/radius evolution. Additionally, the dependence of the kernels on the particle-to-medium impedance ratio is also presented.

On having evaluated the pressure evolution, equations for the temporal variation of particle volume and density are discussed in Sec. IV. The reduction of the present model to the linearized Rayleigh-Plesset equation in the limit of (i) linear approximation and (ii) incompressible ambient is discussed in Sec. V. As a consequence, we compare the Rayleigh-Plesset equation with our linear formulation and asses the effects of non-linearity. In Sec. VI, we apply the present pressure model to predict the pressure inside a finite-sized aluminum particle subjected to normal shock waves of varying strengths and compare against the direct numerical simulation results [31]. Finally conclusions are presented in Sec. VII.

II.   ACOUSTIC SOLUTION

Our interest in this section is to obtain an equation for the time evolution of volume-averaged pressure within a spherical medium (particle, droplet or bubble) in terms of the undisturbed macroscale flow of the continuous phase which will be taken to be varying both in time and space on the scale of the sphere. We will solve the linearized compressible viscous Navier-Stokes equations both inside and outside the sphere with appropriate matching at the interface. To linear approximation the arbitrary time and space dependent ambient flow approaching the sphere can be considered as a superposition of planar waves. Thus, we start with the classical problem of an incident planar sound wave in a viscous compressible, but otherwise stationary, medium scattered by a sphere of finite radius. The incident and the disturbance fields are described by the compressible Navier-Stokes equations:

$$\frac{\partial \rho}{\partial t} + \boldsymbol{\nabla} \cdot (\rho \mathbf{u}) = 0 \,, \tag{3}$$

$$\frac{\partial (\rho \mathbf{u})}{\partial t} + \boldsymbol{\nabla} \cdot (\rho \mathbf{u} \mathbf{u}) = \boldsymbol{\nabla} \cdot \boldsymbol{\sigma} \,, \tag{4}$$

where, $\boldsymbol{\sigma}$ is the stress-tensor and defined as:

$$\boldsymbol{\sigma} = \left[-p\boldsymbol{I} + \mu \left(\boldsymbol{\nabla} \mathbf{u} + (\boldsymbol{\nabla} \mathbf{u})^{\mathrm{T}} \right) + \left(\mu_b - \frac{2}{3}\mu \right) (\boldsymbol{\nabla} \cdot \mathbf{u}) \boldsymbol{I} \right] \,. \tag{5}$$

In the above equations, ρ is the fluid density, p is the pressure, $\mathbf{u}$ represents velocity, μ and μ_b denote the dynamic and bulk viscosities of the medium respectively, t represents time, while $\boldsymbol{I}$ and superscript T are the identity tensor and transpose operator respectively.

In literature, most elementary discussions [32, 33] on acoustic wave solutions involve only homogeneous and stationary medium. However, since we are interested in accounting for inhomogeneous ambient, the background medium (before the passage of the acoustic wave) is allowed to be a function of space and time. In addition, since we are considering a plane (one-dimensional) traveling wave, the background flow variation is restricted to be only in the direction of the wave. Further, in order to limit ourselves to linearized flows, we assume the background to be non-moving. These conditions allow us to express the flow-field as the sum of the base or background flow $(\rho_0, p_0, \mathbf{u}_0 = 0)$ and perturbation flow $(\rho_1, p_1, \mathbf{u}_1)$. In

other words:

$$\rho(\mathbf{r}, t) = \rho_0(\mathbf{r}, t) + \rho_1(\mathbf{r}, t), \quad p(\mathbf{r}, t) = p_0(\mathbf{r}, t) + p_1(\mathbf{r}, t), \quad \mathbf{u}(\mathbf{r}, t) = \mathbf{u}_1(\mathbf{r}, t), \tag{6}$$

where, the suffixes 0 and 1 represent the base and perturbation quantities respectively. Further, the perturbation field can be written as linear superposition of the incident and scattered components. Therefore the flow-field can be viewed as a summation of the undisturbed flow $(Q_0 + Q_1^{\mathrm{in}})$ and disturbed flow (Q_1^{sc}), where Q could represent density, velocity or pressure. The superscripts, 'in' and 'sc', indicate flow properties concerning the incident and scattered fields in general. On substituting Eq. (6) in Eqs. (3) - (4) and linearizing, the first-order equations are given by:

$$\frac{\partial \rho_1}{\partial t} + \boldsymbol{\nabla} \cdot (\rho_0 \mathbf{u}_1) = 0 \,, \tag{7}$$

$$\frac{\partial (\rho_0 \mathbf{u}_1)}{\partial t} = \boldsymbol{\nabla} \cdot \left[-p_1 \boldsymbol{I} + \mu \left(\boldsymbol{\nabla} \mathbf{u}_1 + (\boldsymbol{\nabla} \mathbf{u}_1)^{\mathrm{T}} \right) + \left(\mu_b - \frac{2}{3} \mu \right) (\boldsymbol{\nabla} \cdot \mathbf{u}_1) \boldsymbol{I} \right] . \tag{8}$$

Solutions can readily be found in literature for homogeneous background flows [34–36]. Nevertheless, to employ the same technique in the present context of non-uniform background medium we define a density-weighted velocity [37]:

$$\mathbf{w}_1 = \frac{\rho_0 \mathbf{u}_1}{\rho_{\mathrm{ref}}} \,, \tag{9}$$

where, ρ_{ref} is some constant reference density. However this leads to density appearing in the viscous terms as well. To overcome this, we assume the kinematic viscosity (ν) of the fluid to be a constant such that:

$$\mu = \frac{\rho_0 \mu_{\mathrm{ref}}}{\rho_{\mathrm{ref}}} \quad \text{and} \quad \mu_b = \frac{\rho_0 \mu_{b_{\mathrm{ref}}}}{\rho_{\mathrm{ref}}} \,, \tag{10}$$

where, μ_{ref} and $\mu_{b_{\mathrm{ref}}}$ are reference dynamic and bulk viscosities respectively (also taken to be constants). Substituting Eqs. (9) and (10) in Eqs. (7) - (8), and assuming the variation

in background density ($\boldsymbol{\nabla}\rho_0$) to be of the order of the perturbation quantities one obtains:

$$\frac{\partial \rho_1}{\partial t} + \rho_{\text{ref}}\boldsymbol{\nabla} \cdot \mathbf{w}_1 = 0 \,, \tag{11}$$

$$\rho_{\text{ref}}\frac{\partial \mathbf{w}_1}{\partial t} = \boldsymbol{\nabla} \cdot \left[-p_1\boldsymbol{I} + \mu_{\text{ref}}\left(\boldsymbol{\nabla}\mathbf{w}_1 + (\boldsymbol{\nabla}\mathbf{w}_1)^{\text{T}}\right) + \left(\mu_{b_{\text{ref}}} - \frac{2}{3}\mu_{\text{ref}}\right)(\boldsymbol{\nabla} \cdot \mathbf{w}_1)\boldsymbol{I} \right] \,. \tag{12}$$

We place no restriction on the base state and thus p_0 and ρ_0 can be related by any equation of state appropriate for the material. However, we require the perturbation density and pressure to be related by the constant ambient speed of sound (a_0) corresponding to the base state:

$$p_1 = a_0^2\rho_1 \,. \tag{13}$$

The generality of the present approach to any arbitrary equation of state for the base flow will become important later when we consider the average thermal evolution inside the sphere. Now, Eqs. (11) - (13) resemble the equations governing uniform background flows. For the purposes of this study, the flow properties corresponding to the carrier and dispersed phases will be represented by the superscripts c and d respectively. Subsequently, the density-weighted velocity field can be expressed in terms of the Helmholtz decomposition:

$$\mathbf{w}_1^l = \boldsymbol{\nabla}\phi^l + \boldsymbol{\nabla}\times\Psi^l \,, \tag{14}$$

where, the superscript, l could either represent the carrier/continuous (c) or dispersed (d) phase, ϕ^l represents the scalar velocity potential and Ψ^l is the vector velocity potential. It is important to reiterate that any first order quantity of the outside fluid may be written as the sum of an incident and scattered quantities - i.e., for example, $\mathbf{w}_1^c = \mathbf{w}_1^{\text{in}} + \mathbf{w}_1^{\text{sc}}$. Now, we consider a plane wave propagating in the axial direction (z) and given by:

$$\mathbf{w}_1^{\text{in}}(\omega) = w_1^{\text{in}}\mathbf{e_z} = \exp\{i(k^c z - \omega t)\}\mathbf{e_z} \,, \tag{15}$$

where, $\mathbf{e_z}$ denotes the unit vector in the axial direction, ω is the angular frequency of the incident acoustic wave, which is related via the ambient speed of sound to its wavenumber

k^c, which in turn is given by:

$$k^c = \frac{\omega}{a_0^c}\left[1 - \frac{\mathrm{i}\omega\nu^{c\,2}}{a_0^c}\left(\frac{\mu_{b\mathrm{ref}}^c}{\mu_{\mathrm{ref}}^c} + \frac{4}{3}\right)\right]^{-\frac{1}{2}}. \tag{16}$$

Subsequently, the incoming potential can be written in spherical coordinates as [38],

$$\phi^{\mathrm{in}} = \sum_{n=0}^{\infty} \mathcal{A}_n(2n+1)\mathrm{i}^n j_n(k^c r)P_n(\cos\theta)\mathrm{e}^{-\mathrm{i}\omega t}, \tag{17}$$

where, j_n represents spherical Bessel function of the first kind of order n, P_n denotes Legendre polynomials of the first kind of degree n, $\mathcal{A}_n$ represents the complex amplitude of the incoming wave. Here, r and θ represent the radial and circumferential directions respectively. Similarly the scattered scalar wave potential can be described as [39],

$$\phi^{\mathrm{sc}} = \sum_{n=0}^{\infty} \mathcal{A}_n(2n+1)\mathrm{i}^n S_n^c h_n(k^c r)P_n(\cos\theta)\mathrm{e}^{-\mathrm{i}\omega t}, \tag{18}$$

where, h_n is the spherical Hankel function of the first kind of order n. For the inside flow however, the constraint that the flow needs to be bounded at the origin leads to:

$$\phi^d = \sum_{n=0}^{\infty} \mathcal{A}_n(2n+1)\mathrm{i}^n S_n^d j_n(k^d r)P_n(\cos\theta)\mathrm{e}^{-\mathrm{i}\omega t}, \tag{19}$$

where,

$$k^d = \frac{\omega}{a_0^d}\left[1 - \frac{\mathrm{i}\omega\nu^{d\,2}}{a_0^d}\left(\frac{\mu_{b\mathrm{ref}}^d}{\mu_{\mathrm{ref}}^d} + \frac{4}{3}\right)\right]^{-\frac{1}{2}}. \tag{20}$$

Considering the fact we are dealing with an axisymmetric problem, the vector potential Ψ^l can be reduced to a scalar potential ψ^l that satisfies:

$$\nabla^2\psi^l + k_\nu^{l\,2}\psi^l = 0, \tag{21}$$

where, $k_\nu^l = (1+\mathrm{i})/\delta^l = \sqrt{\mathrm{i}\omega/\nu^l}$, with δ^l denoting the momentum boundary layer thickness and $\nabla^2 = \boldsymbol{\nabla}\cdot\boldsymbol{\nabla}$. The solution of Eq. (21) yields:

$$\psi^l = \sum_{n=0}^{\infty} \mathcal{A}_n(2n+1)\mathrm{i}^n S_{\nu n}^l h_n(k_\nu^l r)P_n(\cos\theta)\mathrm{e}^{-\mathrm{i}\omega t}. \tag{22}$$

11

In Eqs. (18), (19) and (22), S_n^c, S_n^d and $S_{\nu n}^l$ are known as the scattering coefficients which are evaluated using the boundary conditions at the surface of the sphere. Once the scattering coefficients are computed, the complete flow-field can be described.

A. Boundary Conditions

In this study, we only allow for radial pulsations and all other deformations of the sphere surface are ignored. Subsequently, noting that the $n = 0$ (monopole) term accounts purely for the radial pulsation, we segregate the boundary conditions as (i) applicable to $n = 0$ and (ii) applicable to $n \neq 0$. Since for $n = 0$ the flow is independent of θ (independent of viscosity), the scattering coefficients, $S_{\nu_0}^c$ and $S_{\nu_0}^d$ are rendered irrelevant. As a consequence, we only need two interface matching conditions given by,

$$w_{1r}^c\Big|_{n=0} = w_{1r}^d\Big|_{n=0}, \qquad\qquad \text{at } r = R_0\,, \qquad (23a)$$

$$\sigma_{1rr}^c\Big|_{n=0} = \sigma_{1rr}^d\Big|_{n=0} - p_1^{ST}\Big|_{n=0}, \qquad\qquad \text{at } r = R_0\,, \qquad (23b)$$

where, $w_{1r}^c(w_{1r}^d), \sigma_{1rr}^c(\sigma_{1rr}^d)$ and p^{ST} denote the carrier (dispersed) phase radial velocity, normal shear stress of the carrier (dispersed) phase and the surface tension pressure respectively. It must be noted that, before the acoustic wave is incident on the particle, equilibrium conditions exist, such that

$$p_0^c = p_0^d - p_0^{ST}\,, \qquad (24)$$

where, $p_0^{ST} = 2\Gamma/R_0$, is the equilibrium surface tension pressure, with Γ denoting the surface tension coefficient. Similarly, p_0^c and p_0^d represent the equilibrium hydrostatic pressures outside and inside the particle respectively.

Note that the purpose of this study is to obtain an expression for the time-dependent variation of the volume-averaged pressure inside the sphere in terms of the undisturbed flow properties. Since the pressure variation corresponds to the monopole behavior, the analysis of non-monopole modes is unnecessary for the current purposes. However, we present them here for the sake of completeness. For all non-monopole modes ($n \neq 0$), at the interface of the two fluids, the normal and tangential velocities must match. Ignoring variation in surface tension all along the interface, we assume the normal and tangential stresses to be

12

identical. These can quantitatively be written as, at $r = R_0$,

$$w_{1r}^c = w_{1r}^d \, ; \qquad w_{1\theta}^c = w_{1\theta}^d \, ; \qquad \sigma_{1rr}^c = \sigma_{1rr}^d \, ; \qquad \sigma_{1r\theta}^c = \sigma_{1r\theta}^d \, , \tag{25}$$

where, $w_{1\theta}^c(w_{1\theta}^d)$ and $\sigma_{1r\theta}^c(\sigma_{1r\theta}^d)$ correspond to the tangential velocity and shear stress of the particle (medium) respectively. It should be noted that the boundary conditions (Eqs. (23a), (23b) (25)) are applied at the mean radius of the sphere, R_0 as opposed to the instantaneous radius, $R(t)$. However, we argue that this approximation is valid in the linear framework under consideration and such an approximation has been carried out in the past [40–42].

B. Scattering Coefficients

The general expression for the velocity and stress components (with $\mu_{b\mathrm{ref}} = 2\mu_\mathrm{ref}/3$) in terms of the scalar and vector potentials is given as,

$$w_{1r}^l = \frac{\partial \phi^l}{\partial r} - \left[r\nabla^2 - \frac{1}{r}\frac{\partial}{\partial r}r^2\frac{\partial}{\partial r} \right]\psi^l \, ; \tag{26}$$

$$w_{1\theta}^l = \frac{\partial \phi^l}{\partial \theta} + \left[\frac{1}{r}\frac{\partial}{\partial r}r\frac{\partial}{\partial \theta} \right]\psi^l \, ; \tag{27}$$

$$\sigma_{1rr}^l = \rho_\mathrm{ref}^l\frac{\partial \phi^l}{\partial t} + 2\mu_\mathrm{ref}^l\left[\left(-\nabla^2 + \frac{\partial^2}{\partial r^2} \right)\phi^l + \left(r\frac{\partial^3}{\partial r^3} + 3\frac{\partial^2}{\partial r^2} - r\frac{\partial}{\partial r}\nabla^2 - \nabla^2 \right)\psi^l \right] \, ; \tag{28}$$

$$\sigma_{1r\theta}^l = 2\mu_\mathrm{ref}^l\left[\left(\frac{\partial^2}{\partial r\partial \theta}\frac{1}{r} \right)\phi^l + \left\{ \frac{\partial}{\partial \theta}\left(\frac{\partial^2}{\partial r^2} + \frac{1}{r}\frac{\partial}{\partial r} - \frac{1}{r^2} - \frac{1}{2}\nabla^2 \right) \right\}\psi^l \right] \, . \tag{29}$$

To compute the monopole coefficients using Eqs. (23a) and (23b), the appropriate definitions in Eqs. (26) - (29) are used. However, we also need to express the surface tension pressure in terms of velocity potentials (or radial velocity). Therefore we write, in general,

$$p^{ST} = \frac{2\Gamma}{R} \, . \tag{30}$$

Assuming the amplitude of the oscillation of the sphere (R_ϵ) to be small compared to the mean particle radius, we can write, $R(t) = R_0 + R_\epsilon e^{-i\omega t}$. Substituting this expression of radius in Eq. (30), with $R_\epsilon \ll R_0$, we obtain, up to first-order in R_ϵ,

$$p^{ST} = \frac{2\Gamma}{R_0}\left[1 - \frac{R_\epsilon}{R_0}e^{-i\omega t} \right] \, . \tag{31}$$

13

Further, velocity at the interface due to volume pulsation of the sphere is nothing but,

$$\dot{R} = \frac{\mathrm{d}R}{\mathrm{d}t} = w_{1r}^d\Big|_{n=0}. \tag{32}$$

Also, from the definition of $R(t)$,

$$\dot{R} = -\mathrm{i}\omega R_\epsilon \mathrm{e}^{-\mathrm{i}\omega t} \tag{33}$$

Equating Eqs. (32) and (33), we obtain an expression for R_ϵ. Substituting the resulting expression of R_ϵ in Eq. (31) we obtain,

$$p_1^{ST}\Big|_{n=0} = \left(\frac{2\Gamma/R_0}{\mathrm{i}\omega R_0}\right) w_{1r}^d\Big|_{n=0}, \tag{34}$$

where, p_1^{ST} is a first-oder quantity (in surface tension pressure). On substituting the above expression for $p_1^{ST}\Big|_{n=0}$ in Eq. (23b), one may notice that the boundary conditions for $n = 0$ are completely defined and can be expressed in terms of the velocity potentials.

Since our objective is to obtain an explicit expression for volume-averaged pressure inside the sphere and as stated earlier this quantity depends only on the $n = 0$ mode, we shall rewrite the monopole boundary conditions (neglecting surface tension effects) as:

$$\begin{aligned}
-\widehat{w_{1r}^{sc}} + \widehat{w_{1r}^d} &= \widehat{w_{1r}^{in}} \\
-\widehat{p_1^{sc}} + 2\mu_{ref}^c\frac{\partial\widehat{w_{1r}^{sc}}}{\partial r} + \widehat{p_1^d} - 2\mu_{ref}^d\frac{\partial\widehat{w_{1r}^d}}{\partial r} &= \widehat{p_1^{in}}
\end{aligned} \tag{35}$$

where, flow properties corresponding to mode, $n = 0$, at the sphere surface, $r = R_0$, is denoted with the superscript, $\widehat{}$. In other words, for notational simplicity, we write for example, $w_{1r}|_{r=R_0,n=0} = \widehat{w_{1r}}$. Note that the viscous terms corresponding to the incoming flow have been neglected, as they can be considered to be flow properties away from the sphere where viscous effects are negligible. Now expressing the boundary conditions above in terms of scattering coefficients we have:

$$\begin{bmatrix} f_1 & f_2 \\ g_1 & g_2 \end{bmatrix} \begin{Bmatrix} S_0^c \\ S_0^d \end{Bmatrix} = \begin{Bmatrix} \widehat{w_{1r}^{in}} \\ \widehat{p_1^{in}} \end{Bmatrix}, \tag{36}$$

14

where for simplification purposes, we define the following:

$$f_1 = k^c \mathcal{A}_0 h_1(k^c R_0) \mathrm{e}^{-\mathrm{i}\omega t}, \qquad g_1 = k^c \mathcal{A}_0 \left[-\mathrm{i}\rho_{\mathrm{ref}}^c a_0^c h_0(k^c R_0) + \frac{4\mu_{\mathrm{ref}}^c}{R_0} h_1(k^c R_0) \right] \mathrm{e}^{-\mathrm{i}\omega t},$$

$$f_2 = -k^d \mathcal{A}_0 j_1(k^d R_0) \mathrm{e}^{-\mathrm{i}\omega t}, \qquad g_2 = -k^d \mathcal{A}_0 \left[-\mathrm{i}\rho_{\mathrm{ref}}^d a_0^d j_0(k^d R_0) + \frac{4\mu_{\mathrm{ref}}^d}{R_0} j_1(k^d R_0) \right] \mathrm{e}^{-\mathrm{i}\omega t} . \tag{37}$$

The pressure variation inside the sphere can thus be computed by solving for the scattering coefficients in Eq. (36). Note that the right hand side of Eq. (36) involves the zeroth mode of the incoming density-weighted radial velocity and pressure as source terms, which dictate the inside pressure.

III. VOLUME-AVERAGED PARTICLE PRESSURE

In this section we obtain an expression for the average pressure inside the sphere in terms of the time-dependent variation of the incoming undisturbed ambient flow. We begin by considering the inviscid limit, where the wavenumber, k^l reduces to $k_0^l = \omega/c_0^l$ and $\mu_{\mathrm{ref}}^l = 0$. This leads to, $p_1^d = \rho_{\mathrm{ref}}^d \partial \phi^d / \partial t$. Therefore the volume-averaged pressure inside the sphere due to an incoming wave of a given frequency, ω is:

$$\overline{p_1^d}^V(\omega) = \rho_{\mathrm{ref}}^d \mathrm{i}\omega \mathcal{A}_0 S_{0,\mathrm{inv}}^d \frac{3}{k_0^d R_0} j_1(k_0^d R_0) \mathrm{e}^{-\mathrm{i}\omega t}, \tag{38}$$

where, $\overline{(\cdot)}^V$ represents the quantity, $(\cdot)$ averaged over the sphere volume (based on mean radius) and defined as, $\int_{V^d}(\cdot)\,\mathrm{d}V/V^d$, and the suffix, 'inv' denotes that the corresponding quantities have been computed in the inviscid limit. Our objective here is two fold: (i) to express the inside pressure solely in terms of the undisturbed flow quantities and (ii) to provide an expression that is applicable to any complex incident flow-field as opposed to an incoming wave of a given frequency.

In pursuit of the first goal, we shall replace the dispersed phase scattering coefficient, $S_{0,\mathrm{inv}}^d$ with the carrier phase scattering coefficient, $S_{0,\mathrm{inv}}^c$ using the normal velocity boundary condition. In other words, we undertake the following replacements:

$$S_{0,\mathrm{inv}}^d = \frac{\widehat{w_{1r}^{\mathrm{in}}}}{f_{2,\mathrm{inv}}} - \frac{f_{1,\mathrm{inv}}}{f_{2,\mathrm{inv}}} S_{0,\mathrm{inv}}^c, \qquad \rho_{\mathrm{ref}}^d = \tilde{\rho}\rho_{\mathrm{ref}}^c, \qquad k_0^d = \frac{1}{\tilde{a}} k_0^c, \tag{39}$$

15

where, $\tilde{\rho}$ and $\tilde{a}$ represent particle-to-medium density and speed of sound ratios. Substituting Eq. (39) in Eq. (38) leads to:

$$\overline{p_1^d}^V(\omega) = \rho_{\text{ref}}^c \, \mathrm{i}\omega \frac{3\tilde{\rho}\tilde{a}^2}{k_0^c R_0} \left[\mathcal{A}_0 S_{0,\text{inv}}^c h_1(k_0^c R_0) \mathrm{e}^{-\mathrm{i}\omega t} - \frac{\widehat{w_{1r}^{\text{in}}}}{k_0^c} \right] . \tag{40}$$

Further expanding S_0^c using Eq. (36), we have:

$$\overline{p_1^d}^V(\omega) = \rho_{\text{ref}}^c (\mathrm{i}\omega) \frac{3\tilde{\rho}\tilde{a}^2}{k_0^c R_0} \left[\frac{\frac{1}{k_0^c}\frac{h_0(k_0^c R_0)}{h_1(k_0^c R_0)}}{\tilde{\rho}\tilde{a}\frac{j_0(k_0^c R_0/\tilde{a})}{j_1(k_0^c R_0/\tilde{a})} - \frac{h_0(k_0^c R_0)}{h_1(k_0^c R_0)}} \widehat{w_{1r}^{\text{in}}} + \frac{\frac{1}{\rho_{\text{ref}}^c \mathrm{i}\omega}}{\tilde{\rho}\tilde{a}\frac{j_0(k_0^c R_0/\tilde{a})}{j_1(k_0^c R_0/\tilde{a})} - \frac{h_0(k_0^c R_0)}{h_1(k_0^c R_0)}} \widehat{p_1^{\text{in}}} \right] . \tag{41}$$

Now to allow for any non-uniform flow, we express the zeroth mode (monopole) density-weighted normal velocity and pressure as surface averages of the total incoming velocity and pressure. However since we began with an oncoming flow of a given frequency, the expressions for surface-averaged velocity and pressure will be in the Laplace space, where we define the Laplace variable, $s = -\mathrm{i}\omega$. We argue that the variation in pressure inside the sphere has to depend on the time variation of the surface-averaged pressure and normal velocity at the sphere surface. Therefore it is best to express the volume-averaged interior pressure as a function of $\partial \widehat{w_{1r}^{\text{in}}}/\partial t$ and $\partial \widehat{p_1^{\text{in}}}/\partial t$ as opposed to $\widehat{w_{1r}^{\text{in}}}$ and $\widehat{p_1^{\text{in}}}$ itself. Moreover since the sphere considered here is assumed stationary, $\partial/\partial t$ may be replaced by time derivative following the sphere, denoted by $\mathrm{d}/\mathrm{d}t$. It can be shown that (see Appendix A):

$$\widehat{w_{1r}^{\text{in}}} = \mathscr{L}\left(\overline{w_{1r}^{\text{in}}(\mathbf{r},t)}^S\right), \qquad \widehat{p_1^{\text{in}}} = \mathscr{L}\left(\overline{p_1^{\text{in}}(\mathbf{r},t)}^S\right), \tag{42}$$

where, $w_{1r}^{\text{in}}(\mathbf{r},t) = \mathbf{w}_1^{\text{in}}(\mathbf{r},t) \cdot \mathbf{n}$ is the radial component of the velocity vector; $\mathscr{L}(\cdot)$ denotes the Laplace transform and $\overline{(\cdot)}^S$ represents the quantity, $(\cdot)$ averaged over the sphere surface and defined as, $\int_{S^d}(\cdot)\,\mathrm{d}S/S^d$. In addition to the above transformations and combining $-\mathrm{i}\omega$ with $\widehat{w_{1r}^{\text{in}}}$ and $\widehat{p_1^{\text{in}}}$ in Eq. (41) leads to:

$$\mathscr{L}\left(\overline{p_1^d}^V(t)\right) = \frac{R_0}{a_0^c}G_p\mathscr{L}\left(\frac{\mathrm{d}}{\mathrm{d}t}\overline{p_1^{\text{in}}}^S\right) + R_0 G_w \mathscr{L}\left(\frac{\mathrm{d}}{\mathrm{d}t}\rho_{\text{ref}}^c \overline{w_{1r}^{\text{in}}}^S\right), \tag{43}$$

16

where,

$$G_p = \frac{3i\tilde{\rho}\tilde{a}^2}{\tilde{s}^2} \left[\frac{h_0(i\tilde{s})}{h_1(i\tilde{s})} - \tilde{\rho}\tilde{a}\frac{j_0(i\tilde{s}/\tilde{a})}{j_1(i\tilde{s}/\tilde{a})} \right]^{-1}, \qquad G_w = \frac{-3\tilde{\rho}\tilde{a}^2}{\tilde{s}^2} \frac{h_0(i\tilde{s})}{h_1(i\tilde{s})} \left[\frac{h_0(i\tilde{s})}{h_1(i\tilde{s})} - \tilde{\rho}\tilde{a}\frac{j_0(i\tilde{s}/\tilde{a})}{j_1(i\tilde{s}/\tilde{a})} \right]^{-1},$$

(44)

with, $\tilde{s} = sR_0/a_0^c$ being the non-dimensional Laplace variable. Here we define G_p and G_w as the pressure and velocity transfer functions respectively in the Laplace space. Now, noting that (i) $\rho_{\text{ref}}^c w_{1r}^{\text{in}} = \rho_0 u_{1r}^{\text{in}}$ from Eq. (9) and $u_{1r} = u_r$ from Eq. (6), $\rho_{\text{ref}}^c w_{1r}^{\text{in}}$ may be written as $(\rho u_r)^{\text{un}}$ to linear approximation (ii) similarly p_1^{in} may be replaced by p^{un}. Note that the pressure expression derived above is the deviation in pressure from that of the initial base pressure. Therefore the total inside pressure is:

$$\overline{p^d}^V(t) = \overline{p_0^d}^V + \overline{p_1^d}^V(t).$$

(45)

Now taking the Laplace inverse of Eq. (41) leads to a convolution integral and together with Eq. (45), the volume-averaged inside pressure can be written in the time-domain as:

$$\overline{p^d}^V(t) = \overline{p_0^d}^V + \frac{R_0}{a_0^c} \int_{\tilde{\xi}=-\infty}^{\tilde{t}} K_p(\tilde{t}-\tilde{\xi})\frac{\mathrm{d}}{\mathrm{d}t}\overline{p^{\text{un}}}^S \bigg|_{\tilde{t}=\tilde{\xi}} \mathrm{d}\tilde{\xi} + R_0 \int_{\tilde{\xi}=-\infty}^{\tilde{t}} K_w(\tilde{t}-\tilde{\xi})\frac{\mathrm{d}}{\mathrm{d}t}\overline{(\rho u_r)^{\text{un}}}^S \bigg|_{\tilde{t}=\tilde{\xi}} \mathrm{d}\tilde{\xi},$$

(46)

where, $\tilde{t} = ta_0^c/R_0$ and $\tilde{\xi} = \xi a_0^c/R_0$. Further, $K_p = \mathscr{L}^{-1}(G_p)$ and $K_w = \mathscr{L}^{-1}(G_w)$ are the pressure and velocity kernels and $\mathscr{L}^{-1}$ denotes the Laplace inverse operator.

Finally, the effects of viscosity both inside and outside the sphere can be included. In Eq. (39) the complete expressions for f_1, f_2, k^l and S_0^l are used instead of the inviscid counterparts and the process detailed above is repeated. This results in identically the same expression as in Eq. (46) except that the transfer functions are modified by the viscosity ratio ($\tilde{\mu} = \tilde{\rho}\nu^d/\nu^c$) and are given by:

$$\begin{aligned}
G_p &= \frac{3i\tilde{\rho}\tilde{a}^2}{\tilde{s}^2} \left[\frac{h_0(i\tilde{s})}{h_1(i\tilde{s})} - \tilde{\rho}\tilde{a}\frac{j_0(i\tilde{s}/\tilde{a})}{j_1(i\tilde{s}/\tilde{a})} + \frac{4i}{Re}(1-\tilde{\mu}) \right]^{-1}, \\
G_w &= \frac{-3\tilde{\rho}\tilde{a}^2}{\tilde{s}^2} \left[\frac{h_0(i\tilde{s})}{h_1(i\tilde{s})} + \frac{4i}{Re} \right] \left[\frac{h_0(i\tilde{s})}{h_1(i\tilde{s})} - \tilde{\rho}\tilde{a}\frac{j_0(i\tilde{s}/\tilde{a})}{j_1(i\tilde{s}/\tilde{a})} + \frac{4i}{Re}(1-\tilde{\mu}) \right]^{-1},
\end{aligned}$$

(47)

where, $Re = a_0^c R_0/\nu^c$ is the sphere Reynolds number based on the carrier phase speed of sound. The corresponding kernels K_p and K_w to be used in (46) are obtained from the

Laplace inverse of the above viscous transfer functions.

A. Pressure and Velocity Kernels

Equation (46) for volume-averaged pressure inside the sphere is analogous to the evolution equations (1) for the velocity and (2) for the temperature. However the pressure equation (46) is somewhat more complicated by the convolution integrals and can be interpreted in the following way. The perturbation pressure $\overline{p^d}^V(t) - \overline{p_0^d}^V$ has two contributions, one from the ambient pressure variation and the other form the time variation of ambient density-weighted velocity. A step change (denoted by Δ) in the undisturbed ambient pressure averaged over the surface of the sphere (i.e., $\mathrm{d}\overline{p^{\mathrm{un}}}^S/\mathrm{d}t = (a_0^c/R_0)\,\Delta p\,\delta(\tilde{t} - \tilde{\xi}))$ will result in a pressure variation of $\overline{p^d}^V(t) = \overline{p_0^d}^V + \Delta p K_p$, with δ denoting the Dirac-delta function. Similarly a step change in the undisturbed ambient density-weighted velocity averaged over the surface of the sphere (i.e., $\mathrm{d}\overline{(\rho u_r)^{\mathrm{un}}}^S/\mathrm{d}t = (a_0^c/R_0)\,\Delta(\rho u_r)\,\delta(\tilde{t} - \tilde{\xi}))$ will result in a pressure variation of $\overline{p^d}^V(t) = \overline{p_0^d}^V + \Delta(\rho u_r)a_0^c\,K_w$. Thus, the kernels K_p and K_w can be interpreted as response to unit step change in the undisturbed ambient pressure and density-weighted velocity respectively.

With this interpretation, we now explore the temporal behavior of the kernels, K_p and K_w. Note that the transfer functions G_p and G_w defined in Eq. (47) depend only the following four parameters: (i) $\tilde{\rho}$ particle-to-medium density ratio, (ii) $\tilde{a}$ particle-to-medium speed of sound ratio, (iii) $\tilde{\mu}$ particle-to-medium viscosity ratio, and (iv) Re. In the inviscid limit the dependence on the last two parameters are lost. These parametric dependences also apply to the time domain kernel functions K_p and K_w. The reference density and speed of sound of the various materials considered in the present analysis are summarized in table I. In particular, in Sec. VI, we consider shock propagation over an aluminum particle situated in nitromethane. The density and speed of sound ratios are listed in table II for the nitromethane-aluminum and air-aluminum combinations in addition to sand in water and air bubble in water conditions relevant for underwater applications.

The kernels are obtained by numerically computing the inverse Laplace transform [43, 44] of Eq. (44) and are plotted in Fig. 1 for the cases mentioned in table II as a function of dispersed-phase time, $\tilde{t}_d = t a_0^d/R_0$. As can be seen from Fig. 1, the kernels are problem dependent (arising from dependence on $\tilde{\rho}$ and $\tilde{a}$) and need to be recomputed if a different

18

TABLE I: Properties of the dispersed and carrier phases considered in this study.

Material	ρ_0 (kg/m^3)	a_0 (m/s)
Air	1.21	343.23
Water	1000	1482
Nitromethane	982	1647
Aluminum	2783	5350
Sand	2600	1780

TABLE II: Particle-to-medium density ratio, speed of sound ratio, amplitude and time-period of oscillation of the kernels K_p, K_w of the various particle-continuous phase combinations considered in this study.

Medium - Particle	$\tilde{\rho}$	$\tilde{a}$	R_0	$\widetilde{\mathbb{T}}$	$\widetilde{\mathbb{A}}$	
					K_p	K_w
Nitromethane - Aluminum	2.84	3.25	5 μm	2	1.4655	-1.21
Air - Aluminum	2311.16	15.59	40 mm	2	1.5	-1.439
Water - Sand	2.60	1.20	2 mm	2	1.4595	-0.9077
Water - Air	1.21 $\times 10^{-3}$	0.232	4 μm	104	1.978	-0.0137

particle and/or ambient material is considered for example. Nevertheless the late time behavior ($\tilde{t}_d \to \infty$) is problem independent and K_p, K_w reach 1 and 0 respectively as can be seen from Figs. 1(c). It will be shown analytically later in Sec. V A that the late time behavior of the kernels (i.e., $K_p \to 1$, $K_w \to 0$) are the same irrespective of the particle-medium combination chosen.

For the different particle-medium combinations considered, the first maxima ($\widetilde{\mathbb{A}}$) and the non-dimensional time-period of oscillations ($\widetilde{\mathbb{T}}$) of the kernels are listed in table II. The time-scale used to non-dimensionalize the time-period is R_0/a_0^d. It must be noted that for a given dispersed-carrier phase mixture, while $\widetilde{\mathbb{T}}$ is identical for both K_p and K_w, the first maxima depends on the kernel under consideration. Irrespective of the particle-medium combination, the non-dimensional peak value of the pressure kernel is approximately about 1.5. However the first maxima of the velocity kernel varies considerably. For example, as can be seen from Fig. 1(d), for the air bubble in water, since K_w is negligible compared with K_p, only the pressure variation of the external fluid affects the particle pressure and any changes in ambient fluid velocity is immaterial. For the other three cases however, both external pressure and velocity variations are significant.

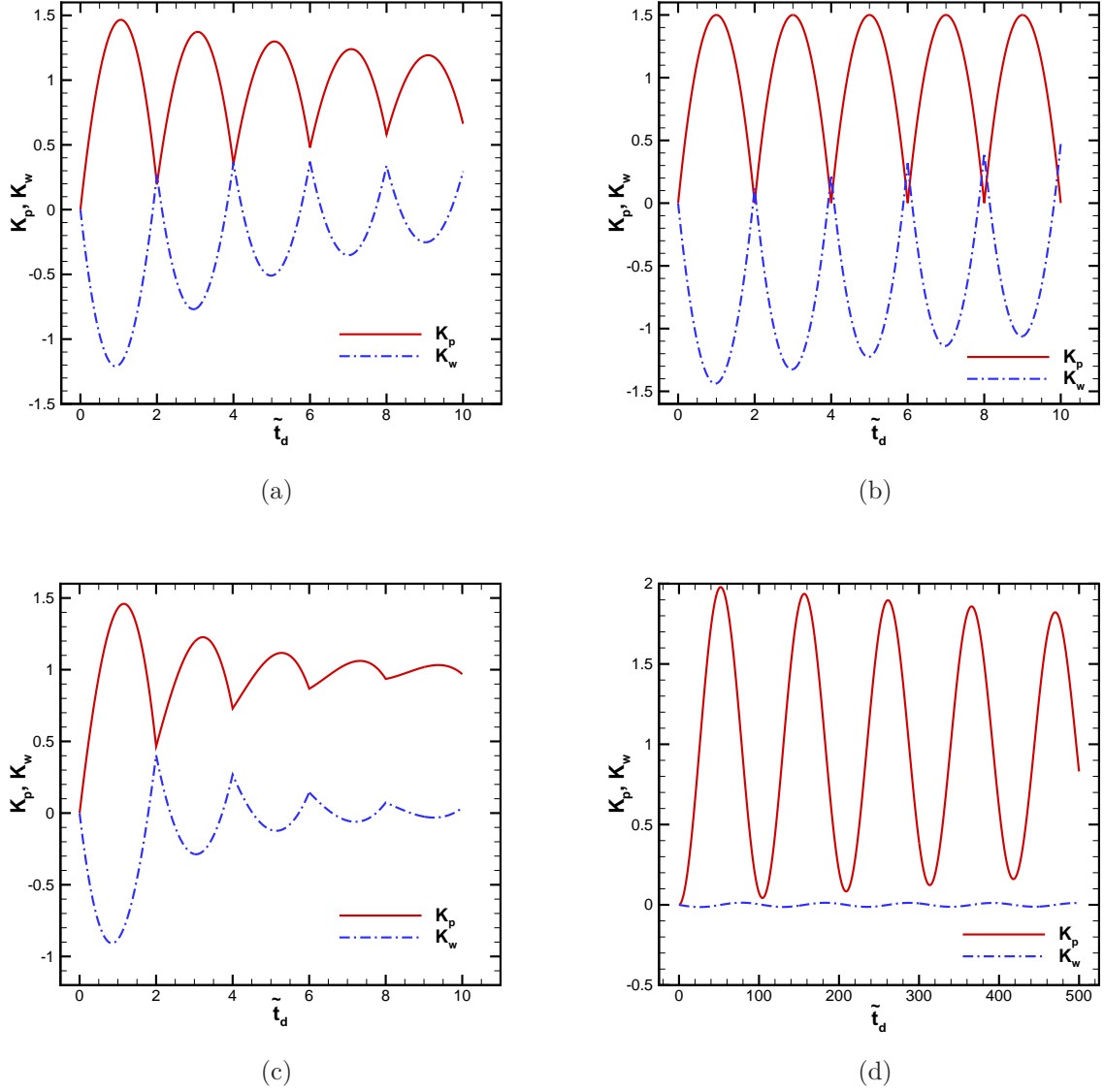As mentioned above, the time-period of oscillation or frequency is the same for both

FIG. 1: Pressure and velocity kernels as a function of non-dimensional particle acoustic time ($\tilde{t}_d$) passing over (a) an aluminum sphere situated in nitromethane with $\tilde{\rho} = 2.84$ and $\tilde{a} = 3.25$ (b) an aluminum sphere situated in air with $\tilde{\rho} = 2311.16$ and $\tilde{a} = 15.59$ (c) a sand particle situated in water with $\tilde{\rho} = 2.6$ and $\tilde{a} = 1.2$ and (d) air bubble in water with $\tilde{\rho} = 1.21 \times 10^{-3}$ and $\tilde{a} = 0.232$. Any viscous effects are neglected.

kernels given a particle-medium combination and the frequency of the kernels are dependent on the impedance ratio, $Z = \tilde{\rho}\tilde{a}$, as shown in Fig. 1. If we consider an acoustic wave sweep past the particle, and if $Z > 1$, $\widetilde{\mathbb{T}}$ is identical to time taken by the acoustic wave within the particle to traverse one particle diameter. Noting that the non-dimensional time taken by an acoustic wave to travel one particle diameter is $\tilde{t}_d = 2$, it can seen from Fig. 1(a)-(c) and

20

table II that $\widetilde{\mathbb{T}} = 2$ for NM-Al, air-Al and water-sand scenarios. This is because for these three cases the impedance ratio is greater than unity. While the frequency of oscillation is a constant provided $Z > 1$, the impedance ratio dictates the decay rate of the kernels. In particular, for the air-Al case, $Z \approx 35000$, for NM-Al combination, $Z \approx 10$ and $Z \approx 3$ for the water-sand scenario, and the decay rate of kernels are found to be inversely proportional to the impedance ratio (Fig. 1). On the other extreme, $Z \ll 1$ for the air bubble in water case, and as can be seen from Fig. 1(d), the contribution of K_w is negligible since $\tilde{\rho}\tilde{a}j_0(i\tilde{s}/\tilde{a})/j_1(i\tilde{s}/\tilde{a}) \ll h_0(i\tilde{s})/h_1(i\tilde{s})$ (Eq. (44)). Moreover the time-period of oscillation is much larger than the other three cases considered. Finally, it is worth mentioning that the time-period of oscillations in the kernels gets translated to the time-period of the particle pressure as will be shown later in Sec. VI for the particular case of NM-Al.

IV.   TIME EVOLUTION OF PARTICLE DENSITY AND VOLUME

In the current analysis, since mass is not allowed to enter or leave the sphere, by mass conservation for the entire sphere:

$$\frac{\partial}{\partial t} \int_{V^d(t)} \rho^d \, dV = 0 . \tag{48}$$

Integrating the above equation in time from $t = 0$ to any time, t, leads to:

$$\widetilde{V^d}(t) = \frac{V^d(t)}{V_0^d} = \left[1 + \frac{\overline{\rho_1^d}^V}{\overline{\rho_0^d}^V} \right]^{-1} , \tag{49}$$

where, V_0^d is the initial volume of the sphere. Since the perturbation density and pressure are linearly related via Eq. (13), we substitute for $\overline{\rho_1^d}^V$ from Eq. (13) in Eq. (49) which, in combination with Eq. (6) yields the time evolution of sphere volume and is given by:

$$\widetilde{V^d}(t) = \left[1 + \frac{\overline{p^d}^V(t) - \overline{p_0^d}^V}{\rho_0^d a_0^{d2}} \right]^{-1} , \tag{50}$$

21

where the expression for $\overline{p^d}^V(t)$ was obtained earlier in Sec. III (Eq. (46)). The inverse of the above equation will yield the density evolution in time and is given by:

$$\overline{\rho^d}^V(t) = \overline{\rho_0^d}^V + \frac{R_0/a_0^c}{a_0^{d2}} \int\limits_{\tilde{\xi}=-\infty}^{\tilde{t}} K_p(\tilde{t}-\tilde{\xi})\frac{\mathrm{d}}{\mathrm{d}t}\overline{p^{\mathrm{un}}}^S\bigg|_{\tilde{t}=\tilde{\xi}} \mathrm{d}\tilde{\xi} \;+\; \frac{R_0}{a_0^{d2}} \int\limits_{\tilde{\xi}=-\infty}^{\tilde{t}} K_w(\tilde{t}-\tilde{\xi})\frac{\mathrm{d}}{\mathrm{d}t}\overline{(\rho u_r)^{\mathrm{un}}}^S\bigg|_{\tilde{t}=\tilde{\xi}} \mathrm{d}\tilde{\xi}\,. \tag{51}$$

V. LIMITING CASES

A. Long-time Behavior

Having obtained an explicit expression for the particle pressure, we now investigate the limiting behavior of the kernels, K_p and K_w. We begin by noting that we are unable to obtain analytical Laplace inverse of the transfers functions G_p and G_w and therefore we resort to numerical inversion [43]. Further, it can be seen that the kernels depend on the density and speed of sound ratios. Since K_p and K_w are responses to unit step change in the incoming pressure and density-weighted normal velocity respectively, let us consider a pressure pulse (with the corresponding density and velocity jump) to impinge on the sphere at time, $t = 0$, such that:

$$\overline{p^{\mathrm{un}}}^S = p_0^c + \Delta p\, H(t)\,, \quad \overline{(\rho u_r)^{\mathrm{un}}}^S = \Delta(\rho u_r)\, H(t)\,, \tag{52}$$

where, p_0^c is the ambient pressure before the impulse and Δp is the jump in pressure after the impulse and $H(t)$ is the Heaviside step function. Let $\Delta(\rho u_r)$ be the corresponding change in the density-weighted normal velocity. Substituting Eq. (52) in Eq. (46) and noting that $\mathrm{d}\overline{p^{\mathrm{un}}}^S/\mathrm{d}t = a_0^c/R_0\Delta p\delta(\tilde{t}-\tilde{\xi})$ leads to:

$$\overline{p^d}^V(t) = \overline{p_0^d}^V + \Delta p\, K_p(\tilde{t}-\tilde{\xi}) + \Delta(\rho u_r)a_0^c K_w(\tilde{t}-\tilde{\xi})\,. \tag{53}$$

22

Let us consider the limiting behavior of the kernels at late times. As $\tilde{t} \to \infty$ ($\tilde{s} \to 0$), the spherical Bessel and Hankel functions appearing in Eq. (44) reduce to:

$$\frac{h_0(i\tilde{s})}{h_1(i\tilde{s})} = \frac{i\tilde{s}}{1+\tilde{s}}, \quad \left.\frac{j_0(i\tilde{s}/\tilde{a})}{j_1(i\tilde{s}/\tilde{a})}\right|_{\tilde{s}\to 0} = \frac{-3i\tilde{a}}{\tilde{s}}. \tag{54}$$

The above substitutions in Eq. (44) lead to:

$$G_p = \frac{1}{\tilde{s}} \implies K_p(\tilde{t}-\tilde{\xi} \to \infty) = 1, \quad G_w = \frac{-1}{1+\tilde{s}} \implies K_w(\tilde{t}-\tilde{\xi} \to \infty) = -e^{-(\tilde{t}-\tilde{\xi})}\bigg|_{\tilde{t}\to\infty} = 0. \tag{55}$$

Substituting Eq. (55) in Eq. (53) we obtain:

$$\overline{p^d}^V(t) = \overline{p_0^d}^V + \Delta p. \tag{56}$$

Therefore we observe from Eq. (56) that the particle pressure eventually equilibrates with that of the carrier phase as it should, since in the absence of surface tension, $\overline{p_0^d}^V = \overline{p_0^c}^V$ from Eq. (24), and Δp is the difference between the post-shock pressure and $\overline{p_0^c}^V$. While the kernels decay exponentially with time, the presence of spherical Bessel functions (which may be written as a combination/summation of trigonometric functions) in the transfer functions will lead to an oscillatory behavior at early and intermediate times as will be shown in Sec. VI. Therefore in summary, any disturbance in the external pressure (and/or normal velocity) will propagate into the particle via sound waves reflecting back and forth inside the sphere/particle before reaching the modified external pressure (caused by the pressure pulse).

B. Reduction to Linearized Rayleigh-Plesset Equation

The pressure equation derived is applicable to any particle subjected to complex incoming flows. The problem of a pulsating spherical bubble in water is of prime importance in the field of underwater explosions and cavitation. Typically in such studies, the dynamic parameter is the bubble radius which is governed by the celebrated Rayleigh-Plesset (RP) equation. The bubble radius is in turn related to the pressure inside the bubble. While the work by Rayleigh [25] ignores the effect of interface surface tension and viscosity of the carrier

fluid, a discussion including these effects can be found in the classic review article by Plesset & Prosperetti [45]. The reader is referred to the works of Leighton [46] and Brennen [23] for a detailed analysis in addition to the work of Prosperetti & Lezzi [19] that discusses the effects of compressibility. The classic nonlinear RP equation in the limit of negligible surface tension and vapor pressure is given by:

$$\frac{p_L - p_\infty}{\rho_0^c} = R\ddot{R} + \frac{3}{2}\dot{R}^2 + \frac{4\nu^c \dot{R}}{R}, \tag{57}$$

where, $p_L = p^c(r = R)$ since we assume surface tension $\Gamma = 0$, and $p_\infty = p^{\text{in}}(r \to \infty)$. In the above equation, over-dot represents the time derivative following the particle. The above equation is derived from first principles and does not linearize the governing equations. However, the bubble pressure is explicitly specified by assuming the interior to be an adiabatic or isothermal lumped system of constant pressure and only the outside flow is solved assuming incompressibility and spatial variation to be purely in the radial direction.

In comparison, in the present work, we solve the flow both within and outside the spherical particle allowing for compressible effects. Therefore in order to derive the RP equation from our current analysis in terms of bubble radius, we begin by revisiting the boundary conditions. We consider a step change in the ambient fluid pressure causing the undisturbed pressure to be p_∞ for $t > 0$ throughout the medium, while maintaining the ambient fluid to be stationary. Additionally, the viscosity within the air bubble and surface tension are ignored. Subsequently the boundary conditions given in Eq. (35) can be written as:

$$-\widehat{w_{1r}^{\text{sc}}} + \dot{R} = 0 \tag{58a}$$

$$-\widehat{p_1^{\text{sc}}} + 2\mu_{\text{ref}}^c \frac{\partial \widehat{w_{1r}^{\text{sc}}}}{\partial r} + \widehat{p_1^d} = \widehat{p_1^{\text{in}}} \tag{58b}$$

Taking the time derivative of Eq. (58a) by using the definitions in Eq. (18) and (26) as applied to the scattered potential one obtains:

$$-\mathrm{i}\omega f_1 S_0^c = \ddot{R} \tag{59}$$

It must be noted that in obtaining the above expression only the $n = 0$ term survives and as a consequence the viscous portion of the scattered potential (ψ) is rendered irrelevant.

Further, using the definition, $p_1^{\text{sc}} = \rho_{\text{ref}}^c \partial \phi^{\text{sc}} / \partial t$ and substituting Eq. (59) in Eq. (58b), we obtain:

$$\widehat{p_1^d} - \widehat{p_1^{\text{in}}} = \rho_{\text{ref}}^c \left[\frac{1}{k^c R_0} \frac{h_0(k^c R_0)}{h_1(k^c R_0)} \right] R_0 \mathscr{L} \left(\ddot{R} \right) - 2\mu_{\text{ref}}^c \left[k^c R_0 \frac{h_1'(k^c R_0)}{h_1(k^c R_0)} \right] \frac{\mathscr{L} \left(\dot{R} \right)}{R_0} . \tag{60}$$

Since the ambient flow is incompressible, the reference densities and viscosities can be considered to be that of the base flow itself, i.e., $\rho_{\text{ref}}^c = \rho_0^c$ and $\mu_{\text{ref}}^c = \mu_0^c$. Using Eq. (42), we can write, $\widehat{p_1^{\text{in}}} = \mathscr{L} \left(\overline{p_1^{\text{in}}}^S \right)$. Moreover $\mathscr{L} \left(\overline{p_1^{\text{in}}}^S \right) = \mathscr{L} \left(\overline{p_1^{\text{un}}}^S \right) - \mathscr{L} \left(\overline{p_0^c}^S \right)$. In the incompressible limit, i.e., as $a_0^c \to \infty$ any change in pressure at far-field is immediately felt throughout the fluid. As a consequence of this, $\widehat{p_1^{\text{in}}} = \mathscr{L} \left(p_\infty \right) - \mathscr{L} \left(\overline{p_0^c}^S \right)$. Further the incompressibility condition leads to $k^c R_0 \to 0$ and as a result we have:

$$\left. \frac{1}{k^c R_0} \frac{h_0(k^c R_0)}{h_1(k^c R_0)} \right|_{k^c R_0 \to 0} = 1 ; \qquad \left. k^c R_0 \frac{h_1'(k^c R_0)}{h_1(k^c R_0)} \right|_{k^c R_0 \to 0} = -2 . \tag{61}$$

Similar to the expression of $\widehat{p_1^{\text{in}}}$ above and noting that the fluid inside the bubble is considered homogeneous, $\widehat{p_1^d} = \mathscr{L} \left(p^d \right) - \mathscr{L} \left(\overline{p_0^d}^S \right)$. Finally in the absence of surface tension we note that $\mathscr{L} \left(p^d \right) = \mathscr{L} \left(p_L \right)$. From the equality of $\overline{p_0^c}^S$ and $\overline{p_0^d}^S$ we obtain, $\widehat{p_1^d} - \widehat{p_1^{\text{in}}} = \mathscr{L} \left(p_L \right) - \mathscr{L} \left(p_\infty \right)$. Taking the Laplace inverse we finally obtain:

$$\frac{p_L - p_\infty}{\rho_0^c} = R_0 \ddot{R} + \frac{4\nu^c \dot{R}}{R_0} . \tag{62}$$

which precisely is the RP equation in the linear limit. Note that the above equation is linear in bubble radius. In the classic RP equation (Eq. (57)), the term $3\dot{R}^2/2$ arises from the convective term of the Navier-Stokes equation. Since the current work is restricted to linear regime, (i) the non-linear term has been ignored and (ii) the time-dependent radius only appears with the time derivative, while the radius itself otherwise shows up as the mean radius. In both Eqs. (57) and (62), if the gas inside the bubble is assumed to follow adiabatic law, then $p_L = p_0^d (R_0/R)^{3\gamma}$.

As specified earlier, in the current work, we allow for both fluids to be viscous and compressible and thereby allow propagation of both acoustic and viscous waves in both the carrier and dispersed phases. With all such complexities accounted the evolution of bubble

radius follows directly from Eq. (50) and is given by:

$$R(t) = R_0 \left[1 + \frac{\overline{p^d}^V(t) - \overline{p_0^d}^V}{\rho_0^d a_0^{d2}} \right]^{-1/3}, \tag{63}$$

In Eq. (63), the effects of viscosity can be taken into account if the kernels in Eq. (47) are used when evaluating the volume-averaged particle pressure. Note that the bubble radius derived above (Eq. (63)) is expressed in terms of the bubble pressure. However, it is possible to obtain an expression for bubble radius starting from Eq. (33) and purely using the linear theory. The procedure is similar to that outlined in Sec. III, where time derivative of the particle radius is first expressed in terms of dispersed phase flow quantities and then transforming them to flow quantities that depend explicitly on undisturbed properties. Therefore carrying out the above mentioned linear analysis leads to:

$$R(t) = R_0 \left[1 - \frac{R_0/a_0^c}{3\rho_0^d a_0^{d2}} \int\limits_{\tilde{\xi}=-\infty}^{\tilde{t}} K_p(\tilde{t} - \tilde{\xi}) \frac{\mathrm{d}}{\mathrm{d}t} \overline{p^{\mathrm{un}}}^S \bigg|_{\tilde{t}=\tilde{\xi}} \mathrm{d}\tilde{\xi} - \frac{R_0}{3\rho_0^d a_0^{d2}} \int\limits_{\tilde{\xi}=-\infty}^{\tilde{t}} K_w(\tilde{t} - \tilde{\xi}) \frac{\mathrm{d}}{\mathrm{d}t} \overline{(\rho u_r)^{\mathrm{un}}}^S \bigg|_{\tilde{t}=\tilde{\xi}} \mathrm{d}\tilde{\xi} \right].$$

$$\tag{64}$$

It is worth mentioning that Eqs. (63) and (64) are identical in the linear limit. When nonlinear effects are negligible, $\left(\overline{p^d}^V(t) - \overline{p_0^d}^V \right) / \rho_0^d a_0^{d2} \ll 1$. Therefore after substituting Eq. (46) in Eq. (63), we perform a binomial expansion on the right hand side of Eq. (63) and consider only the leading order term, neglecting higher order terms. The resulting expression is the same as that of Eq. (64). However, it must be noted that Eq. (63) is only approximate and therefore in the current work, Eq. (64) is used to compute the instantaneous particle radius.

Now we consider the example provided in Ref. 47 of a time-varying ultrasound wave impinging on an air bubble in water and compare the bubble radius obtained using Eqs. (57), (62) and (64). The initial bubble radius (R_0) is 2 mm, the pressure in the carrier phase is sinusoidally varied as, $p_\infty = p_0^c - p_a \cos(2\pi f t)$ with $p_0^c = p_0^d = 1$ atm and $p_a = 2.7$ atm. The frequency of the driving pressure, $f = 10$ kHz, the dynamic viscosities of water and air are taken to be 10^{-2} poise and 1.8×10^{-4} poise respectively. The air is taken to be adiabatic with $\gamma = 1.4$, while the effects of surface tension are ignored. All of the above parameters are taken from Ref. 47. As can be seen from Fig. 2, the linearized Rayleigh-Plesset equation (Eq. (62) obtained from our analysis by solving only the carrier phase in the incompressible
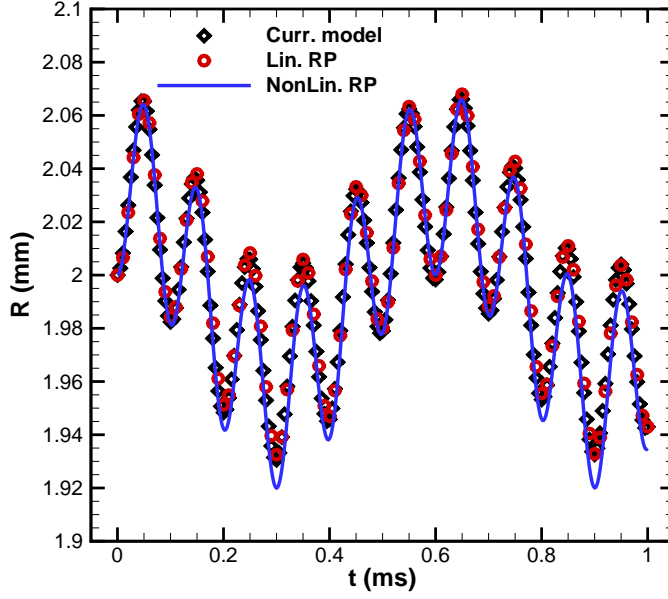
FIG. 2: The time evolution of bubble radius initially at 2 mm subjected to a driving frequency of 10 kHz and amplitude of 2.7 atm. The base pressures in the medium and air bubble are both taken to be 1 atm. The other parameters are $\gamma = 1.4$, $\mu_{\text{ref}}^c = 10^{-3}$, $\mu_{\text{ref}}^d = 1.8 \times 10^{-5}$ and $\Gamma = 0$.

limit) is in good agreement with the model that takes into account details of the acoustic and viscous waves traveling within and outside the particle. The results compare well even with the classical non-linear RP equation (Eq. (57)) except at certain time instances when non-linearity becomes important.

To study the behavior of a much smaller bubble, where the effects of non-linearity becomes prominent the application of the present model with either Eq. (63) or (64) requires some care. As the bubble base pressure (p_0^d) in itself varies substantially over time, one needs to first obtain the time-evolving base density (ρ_0^d) and speed of sound (a_0^d). Subsequently, these base quantities must be fed to compute the kernel, which now become parametrically time-dependent. In other words, the density ratio ($\tilde{\rho}$) and speed of sound ratio ($\tilde{a}$) that determine the kernels to be used in Eq. (46) for the volume-averaged pressure or in Eq. (64) for the bubble radius, are themselves time varying. As a consequence the evaluation of the convolution integral becomes more involved, where the kernels have to be updated at every time instant as ρ_0^d and a_0^d changes over time.

TABLE III: Pre- and post-shock properties of air and nitromethane for the varying shock Mach numbers (M_s) considered.

Medium	M_s	Post-shock properties			Pre-shock properties		
		p (MPa)	ρ (kg/m^3)	u (m/s)	p (MPa)	ρ (kg/m^3)	u (m/s)
NM	1.11	200	1045.6	111.3	0.101325	982	0
	1.25	500	1116.9	248.0	0.101325	982	0

VI. APPLICATION - SHOCK PROPAGATION OVER A SPHERE

In this section, we consider passage of a planar normal shock wave over a stationary aluminum particle situated in nitromethane to validate our pressure formulation. While the properties of NM, Al are detailed in table I, the Mach numbers and their corresponding post-shock properties under study are tabulated in table III. Note that size of the aluminum particle (5 μm radius) and the post-shock properties are taken from Ref. 31. Nevertheless there are two important differences worth mentioning. First, the time evolution of the various dispersed phase quantities presented in Ref. 31 are averaged over the particle mass; however these are transformed to volume-averaged quantities to compare against the current analysis. Second, the simulations presented in Ref. 31 are re-run by taking both NM and Al to follow the stiffened gas EOS. The reader is referred to Ref. 48 for a brief overview of the stiffened gas EOS used in these simulations. While the simulations allow for shape changes, the model/theory considered here assumes the particle to remain spherical and allows only for volumetric pulsations without any shape change. The viscous effects are neglected in this context and therefore $\tilde{\mu} = 0$.

We begin by considering a planar shock propagation over an aluminum particle in nitromethane. The volume-averaged particle pressure is computed using Eq. (46). The necessary kernels (K_p, K_w) have been computed and presented in Fig. 1(a). For the NM-Al case under consideration, the pre-shock ambient pressure and the initial volume-averaged interior pressure $\left(\overline{p_0^d}^V\right)$ is chosen to be 0.1 MPa. Similarly, at time $t = 0$, the particle is said to be in thermal equilibrium with the ambient at 300 K. As the shock wave sweeps over the particle, Fig. 3 shows the time history of $\overline{p^{\mathrm{un}}}^S$ and $\overline{(\rho u_r)^{\mathrm{un}}}^S$ that appear within the integrals in Eq. (46). We can observe that both the surface-averaged pressure and density-weighted radial velocity rapidly increase from their pre-shock to post-shock values on the acoustic scale. Since the kernels also evolve on the acoustic scale, the convolution integral must be

accurately computed (change in $\overline{p^{un}}^S$ and $\overline{(\rho u_r)^{un}}^S$ cannot be assumed to be step functions).

The time evolution of particle pressure is plotted in Fig. 4(a) due to a shock wave of Mach number, $M_s = u_s/a_0^c = 1.11$, where u_s is the shock velocity. The results are plotted as a function of non-dimensional shock time $(\tilde{t}_s)$, defined as tu_s/R_0. Note that as the shock traverses the particle, the volume-averaged particle pressure begins at 0.1 MPa and eventually equilibrates with the post-shock pressure of 0.2 GPa for $\tilde{t}_s \geq 9$. In Fig. 4(a) while the pressure (K_p) contribution is always positive the normal velocity contribution (K_w) becomes both positive and negative over time depending on the direction of pulsation of the particle surface. The sum of these two contributions in addition to the initial interior pressure leads to the time history of the total particle pressure. However it undergoes oscillations as it goes from the pre-shock to post-shock pressure and this arises from the oscillatory kernels and correspond to the waves traveling back and forth inside the particle. If one ignores the oscillatory behavior, the volume-averaged particle pressure can be observed to reach the post-shock pressure exponentially beginning from the initial undisturbed pressure as shown by the black dash-line in Fig. 4. In other words, the non-oscillatory approach to the final pressure can be described by:

$$\overline{p^d}^V = p^{final}\left(1 - \exp(-\tilde{t}_s)\right) + p^{initial}\exp\left(-\tilde{t}_s\right) , \tag{65}$$

where $p^{initial}$ and p^{final} denote respectively the initial and final pressures attained by the particle, which happen to be the pre- and post-shock pressures listed in table III. The above can be rewritten in a form similar to the equation of motion or the temperature evolution equation as:

$$\frac{d\overline{p^d}^V}{dt} = \frac{p^{final} - \overline{p^d}^V}{\tau_{pP}} , \tag{66}$$

where $\tau_{pP} = R_0/u_s$ is the shock propagation time scale.

Also shown in Fig. 4(a) is the comparison of the current model with that of the direct numerical simulation in Ref. 31 and as can be observed the prediction is reasonable. The differences can be attributed to several factors: while the theoretical model developed here is based on linear perturbation assumption, clearly the shock-induced flow around the sphere in the numerical simulation is strongly nonlinear. Furthermore, at the strong post-shock pressure the aluminum particle is observed to undergo some shape deformation, while the
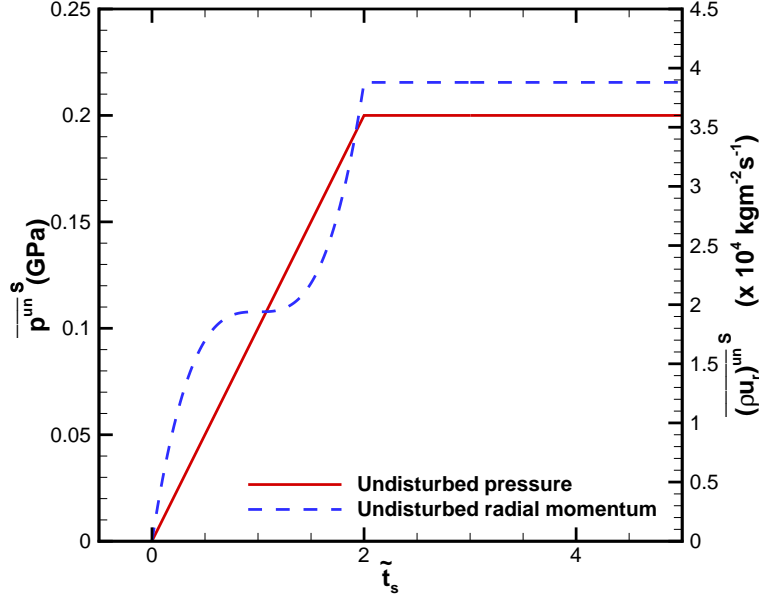
FIG. 3: Undisturbed surface-averaged pressure and radial momentum of the carrier phase as a function of non-dimensional shock time $(\tilde{t}_s)$ as a normal shock of $M_s = 1.11$ traverses an aluminum sphere situated in nitromethane with $\tilde{\rho} = 2.84$ and $\tilde{a} = 3.25$.

theoretical model assumes a spherical shape at all times. Finally the simulations employ a non-ideal gas equation of state, which are not accounted for in the current model of the linearized perturbation flow. The time-period of oscillation based on the shock speed, $\mathbb{T}_s = \Delta t_s R_0 / u_s$, observed both in the simulations and the present model is found to be approximately 1.85 ns. Here Δt_s denotes the difference in shock time between any two successive pressure peaks. The time taken by an acoustic wave inside the particle to travel one diameter is given by, $\mathbb{T} = 2R_0 / a_0^d = 1.87$ ns, which is consistent with the time-period of oscillation, $\mathbb{T}_s$, computed above. The observations made for $M_s = 1.11$ hold true for $M_s = 1.25$ as well and is shown in Fig. 4(b). However the discrepancy between simulation and the pressure model is higher, perhaps owing to increased nonlinearity and the fact that the speed of sound of the ambient and particle used to compute the kernels begins to vary from their base values when a shock of finite strength traverses the sphere.

The density evolution of the dispersed phase as computed from Eq. (51) is plotted in Fig. 5 and the results are in good agreement with the simulations [31]. As can be seen from the figure, the density change is minimal in comparison with the pressure change. Note that the
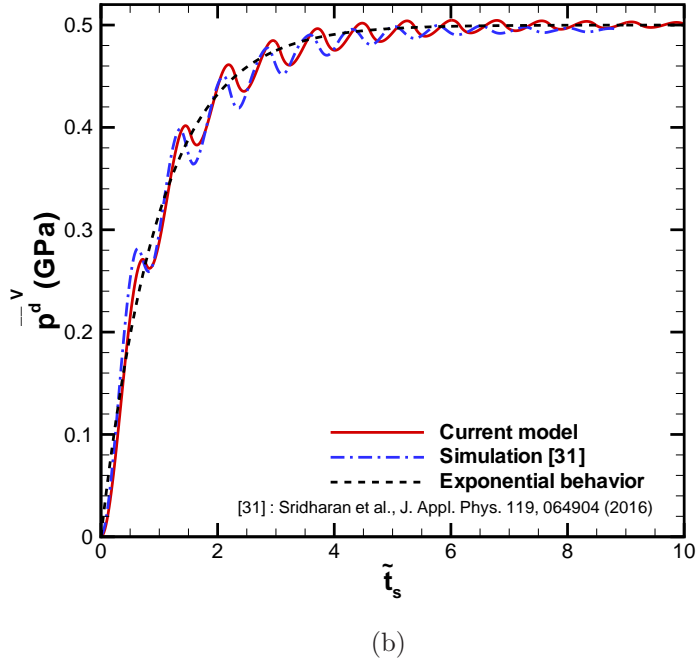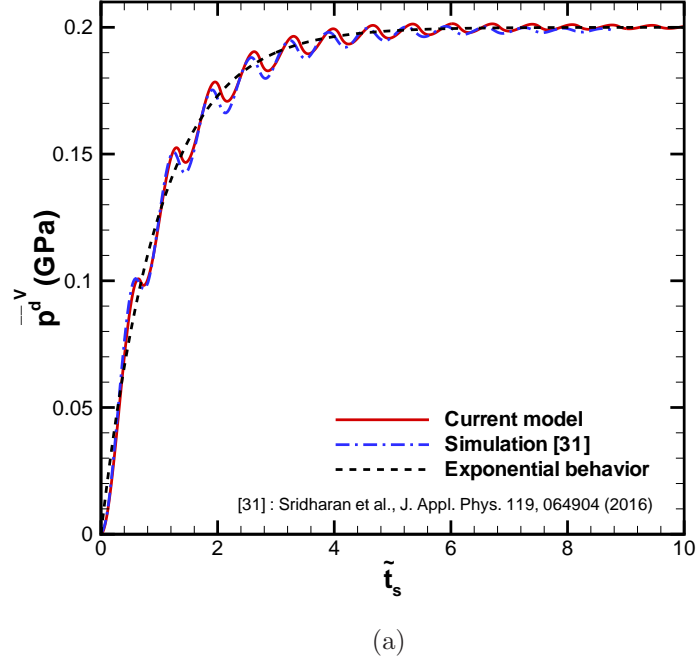
(a)

(b)

FIG. 4: Volume averaged particle pressure as a function of non-dimensional shock time $(\tilde{t}_s)$ for a normal shock of (a) $M_s = 1.11$ and (b) $M_s = 1.25$ passing over an aluminum sphere in nitromethane with $\tilde{\rho} = 2.84$ and $\tilde{a} = 3.25$. Also shown is the comparison of the current pressure formulation with results in Ref. 31.
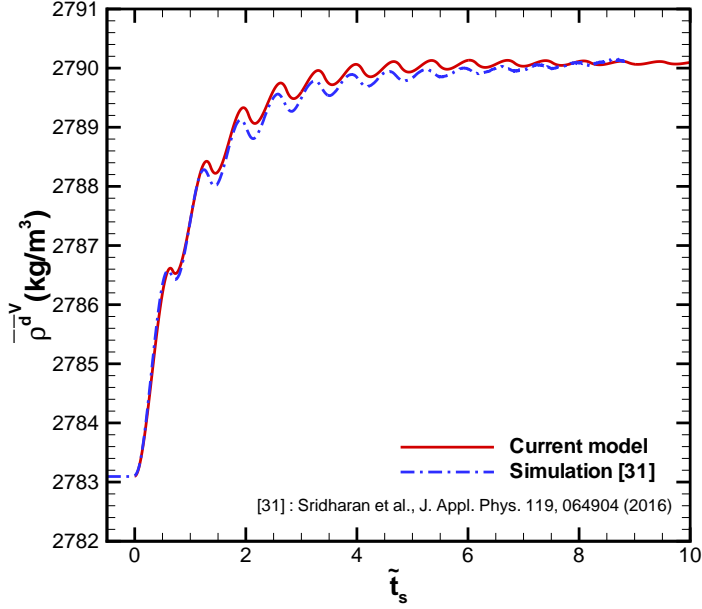
FIG. 5: Volume averaged particle density as a function of non-dimensional shock time $(\tilde{t}_s)$ for a normal shock of $M_s = 1.11$ passing over an aluminum sphere in nitromethane with $\tilde{\rho} = 2.84$ and $\tilde{a} = 3.25$.

particle pressure reaches the post-shock pressure of 0.2 GPa for shock time scales, $\tilde{t}_s \geq 9$, since it is the pressure difference that acts as the driver in our model.

VII. CONCLUSIONS

An equation that models the particle pressure in response to any complex, time-dependent, non-uniform flows in a compressible medium is presented. A plane acoustic wave of a given frequency and wavenumber is assumed to impinge on the particle. The zeroth mode (monopole) of the carrier phase density-weighted normal velocity and pressure were identified as the source terms affecting the particle pressure. Subsequently, the volume-averaged dispersed phase pressure was expressed as a function of density-weighted normal acceleration and time-derivative of the external pressure. The monopole terms were further formulated as surface average of the incoming flow properties thus allowing for any complex incident flow field. A Laplace inverse of the resulting expression was carried out to obtain the pressure expression in the time domain. Analogous to the particle equation

of motion, the pressure was also expressed as a convolution integral, comprising two parts. One arising due to flow unsteadiness, termed the kernel, and two, arising from the spatial flow inhomogeneity. The kernels obtained were found to depend on the particle to medium density ratio ($\tilde{\rho}$), speed of sound ratio ($\tilde{a}$), viscosity ratio ($\tilde{\mu}$) and Reynolds number (Re). A similar equation was also derived to compute the time evolution of particle volume/radius and density. Further, the current formulation reduced to the linearized Rayleigh-Plesset equation in the limit of (i) incompressible medium and (ii) homogeneous flow behavior within the particle. The present formulation was applied to study the pressure history inside an aluminum particle as normal shock waves of varying strengths passed over it; and the results obtained were in good agreement with the direct numerical simulations [31].

Appendix A: Equivalence between the monopole component of radial velocity/pressure and surface-averaged incoming radial velocity/pressure

The radial component of the incoming velocity can be obtained using Eq. (26) as:

$$w_{1r}^{\text{in}} = k^c \sum_{n=0}^{\infty} \mathcal{A}_n (2n+1) \mathrm{i}^n j_n'(k^c r) P_n(\cos\theta) \mathrm{e}^{-\mathrm{i}\omega t} . \tag{A1}$$

Now if we consider only the monopole component of the density-weighted radial velocity above we obtain:

$$\widehat{w_{1r}^{\text{in}}} = \mathcal{A}_0 k^c {j_0}'(kR_0) \mathrm{e}^{-\mathrm{i}\omega t} . \tag{A2}$$

The surface average of the incoming radial velocity can be obtained by integrating Eq. (A1) as:

$$\mathscr{L}\left(\overline{w_{1r}^{\text{in}}(\mathbf{r},t)}^{S}\right) = \frac{1}{2}\mathcal{A}_0 k^c j_0'(kR_0)\mathrm{e}^{-\mathrm{i}\omega t}\int_0^{\pi}\sin\theta\,\mathrm{d}\theta$$

$$= \mathcal{A}_0 k^c {j_0}'(kR_0)\mathrm{e}^{-\mathrm{i}\omega t} . \tag{A3}$$

In obtaining the above expression, we note that of all the terms in the summation in Eq. (A1) only one term ($n = 0$) survives the integration in Eq. (A3). In addition we have used the definition of Legendre polynomial, $P_0(\cos\theta) = 1$. Subsequently, comparing Eqs. (A2) and (A3), we arrive at their equivalence mentioned in Eq. (42).

The pressure equivalence can also be proved as follows. Starting from Eq. (28), the

33

incoming pressure equation can be expressed as:

$$p_1^{\text{in}} = \rho_{\text{ref}}^c \frac{\partial \phi^{\text{in}}}{\partial t} = -\rho_{\text{ref}}^c i\omega \sum_{n=0}^{\infty} \mathcal{A}_n (2n+1) i^n j_n(k^c r) P_n(\cos\theta) e^{-i\omega t} . \tag{A4}$$

The monopole component of Eq. (A4) yields:

$$\widehat{p_1^{\text{in}}} = -\rho_{\text{ref}}^c i\omega \mathcal{A}_0 j_0(kR_0) e^{-i\omega t} . \tag{A5}$$

The surface average of the incoming radial velocity can be obtained by integrating Eq. (A4) and noting only $n = 0$ survives the integration, we obtain:

$$\begin{aligned}
\mathscr{L}\left(\overline{p_1^{\text{in}}(\mathbf{r}, t)}^S\right) &= -\rho_{\text{ref}}^c i\omega \frac{1}{2} \mathcal{A}_0 j_0(kR_0) e^{-i\omega t} \int_0^{\pi} \sin\theta \, d\theta \\
&= -\rho_{\text{ref}}^c i\omega \mathcal{A}_0 j_0(kR_0) e^{-i\omega t} .
\end{aligned} \tag{A6}$$

Thus the equivalence referred to in Eq. (42) has been achieved.

[1] S. Balachandar and John K. Eaton, "Turbulent dispersed multiphase flow," Ann. Rev. Fluid Mech. **42**, 111–133 (2010).

[2] P. G. Saffman, "On the stability of laminar flow of a dusty gas," J. Fluid Mech. **13**, 120–128 (1962).

[3] F. E. Marble, "Dynamics of dusty gases," Ann. Rev. Fluid Mech. **2**, 397–446 (1970).

[4] G. G. Stokes, "On the effect of the internal friction of fluids on the motion of pendulums," Trans. Camb. Phil. Soc. **9**, 8–106 (1851).

[5] A. B. Basset, *A treatise on hydrodynamics* (Deighton, Bell and Company, 1888).

[6] J. Boussinesq, "Sur la résistance qu'oppose un liquide indéfini au repos au mouvement varié d'une sphère solide," C. R. Acad. Sci. Paris **100**, 935–937 (1885).

[7] C. W. Oseen, *Hydrodynamik* (Leipzig:Akademische Verlagsgesellschaft, 1927).

[8] H. Faxén, "Der widerstand gegen die bewegung einer starren kugel in einer zähen flüssigkeit, die zwischen zwei parallelen, ebenen wänden eingeschlossen ist," Arkiv. Mat. Astron. Fys. **18** (1924).

[9] M. R. Maxey and J. J. Riley, "Equation of motion for a small rigid sphere in a nonuniform flow," Phys. Fluids **26**, 883–889 (1983).

[10] R. Gatignol, "The Faxén formulas for a rigid particle in an unsteady non-uniform Stokes-flow," J. Mec. Theor. Appl. **2**, 143–160 (1983).

[11] Seung Man Yang and L. G. Leal, "A note on memory-integral contributions to the force on an accelerating spherical drop at low Reynolds number," Phys. Fluids A: Fluid Dyn. **3**, 1822–1824 (1991).

[12] M. Parmar, A. Haselbacher, and S. Balachandar, "Generalized Basset-Boussinesq-Oseen equation for unsteady forces on a sphere in a compressible flow," Phys. Rev. Lett. **106**, 084501 (2011).

[13] R. Clift and W. H. Gauvin, "The motion of particles in turbulent gas streams," Proc. Chemeca **1**, 14–28 (1970).

[14] A. L. Longhorn, "The unsteady, subsonic motion of a sphere in a compressible inviscid fluid," Q. J. Mech. Appl. Math. **5**, 64–81 (1952).

[15] R. Mei, "History force on a sphere due to a step change in the free-stream velocity," Int. J. Multiph. Flow **19**, 509–525 (1993).

[16] M. Parmar, A. Haselbacher, and S. Balachandar, "On the unsteady inviscid force on cylinders and spheres in subcritical compressible flow," Philos. Trans. Roy. Soc. A **366**, 2161–2175 (2008).

[17] C. Crowe, M. Sommerfeld, and Y. Tsuji, *Multiphase Flow with Droplets and Particles* (CRC Press, 1998).

[18] Andrea Prosperetti, "Bubble dynamics: A review and some recent results," Appl. Sci. Res. **38**, 145–164 (1982).

[19] A. Prosperetti and A. Lezzi, "Bubble dynamics in a compressible liquid. Part 1. First-order theory," J. Fluid Mech. **168**, 457–478 (1986).

[20] Kenneth S. Suslick and David J. Flannigan, "Inside a collapsing bubble: Sonoluminescence and the conditions during cavitation," Ann. Rev. Phys. Chem. **59**, 659–683 (2008).

[21] ShengHsueh Yang, ShenqYuh Jaw, and KehChia Yeh, "Single cavitation bubble generation and observation of the bubble collapse flow induced by a pressure wave," Expt. Fluids **47**, 343–355 (2009).

[22] Werner Lauterborn and Thomas Kurz, "Physics of bubble oscillations," Rep. Prog. Phys. **73**, 106501 (2010).

[23] Christopher E. Brennen, *Cavitation and Bubble Dynamics* (Oxford University Press, 1995).

[24] Michael P. Brenner, Sascha Hilgenfeldt, and Detlef Lohse, "Single-bubble sonoluminescence," Rev. Mod. Phys. **74**, 425–484 (2002).

[25] Lord Rayleigh, "On the pressure developed in a liquid during the collapse of a spherical cavity," Philos. Mag. **34**, 94–98 (1917).

[26] M. S. Plesset, "The dynamics of cavitation bubbles," J. Appl. Mech. **16**, 277–282 (1949).

[27] D. Felipe Gaitan, Lawrence A. Crum, Charles C. Church, and Ronald A. Roy, "Sonoluminescence and bubble dynamics for a single, stable, cavitation bubble," J. Acoust. Soc. Am. **91**, 3166–3183 (1992).

[28] Ritva Löfstedt, Bradley P. Barber, and Seth J. Putterman, "Toward a hydrodynamic theory of sonoluminescence," Phys. Fluids A **5**, 2911–2928 (1993).

[29] A. Prosperetti and Y. Hao, "Modelling of spherical gas bubble oscillations and sonoluminescence," Phil. Trans. Roy. Soc. A **357**, 203–223 (1999).

[30] S. Annamalai and S. Balachandar, "Generalized Faxéns theorem for time-domain force on a sphere in unsteady viscous compressible flows," submitted to J. Fluid Mech. (2016).

[31] P. Sridharan, T. L. Jackson, J. Zhang, S. Balachandar, and S. Thakur, "Shock interaction with deformable particles using a constrained interface reinitialization scheme," J. Appl. Phys. **119**, 064904 (2016).

[32] David T. Blackstock, *Fundamentals of Physical Acoustics* (John Wiley & Sons, 2000).

[33] Mark. F. Hamilton and David. T. Blackstock, eds., *Nonlinear Acoustics* (Academic Press Limited, 1998).

[34] A. A. Doinikov, "Acoustic radiation pressure on a rigid sphere in a viscous-fluid," Proc. R. Soc. A **447**, 447–466 (1994).

[35] Subramanian Annamalai, S. Balachandar, and Manoj K. Parmar, "Mean force on a finite-sized spherical particle due to an acoustic field in a viscous compressible medium," Phys. Rev. E **89**, 053008 (2014).

[36] A. N. Guz, *Dynamics of Compressible Viscous Fluid* (Cambridge Scientific Publishers, 2009).

[37] M. Parmar, A. Haselbacher, and S. Balachandar, "Equation of motion for a sphere in non-uniform compressible flows," J. Fluid Mech. **699**, 352–375 (2012).

[38] T. Hasegawa, "Acoustic radiation force on a sphere in a quasistationary wave field-theory," J. Acoust. Soc. Am. **65**, 32–40 (1979).

[39] T. Hasegawa and K. Yosioka, "Acoustic-radiation force on a solid elastic sphere," J. Acoust. Soc. Am. **46**, 1139–1143 (1969).

[40] K. Yosioka and Y. Kawasima, "Acoustic radiation pressure on a compressible sphere," Acustica **5**, 167–173 (1955).

[41] A. A. Doinikov, "Acoustic radiation pressure on a compressible sphere in a viscous-fluid," J. Fluid Mech. **267**, 1–21 (1994).

[42] Anthony Eller, "Force on a bubble in a standing acoustic wave," J. Acous. Soc. Am. **43**, 170–171 (1968).

[43] Lubomír Brančík, "Utilization of Matlab in simulation of linear hybrid circuits," Radioengineering **12**, 6–11 (2003).

[44] Lubomír Brančík, "MATLAB for Engineers - Applications in Control, Electrical Engineering, IT and Robotics," (InTech, 2011) Chap. Numerical Inverse Laplace Transforms for Electrical Engineering Simulation, pp. 51–74.

[45] M. S. Plesset and A. Prosperetti, "Bubble dynamics and cavitation," Ann. Rev. Fluid Mech. **9**, 145–185 (1977).

[46] T. G. Leighton, "The Rayleigh-Plesset equation in terms of volume with explicit shear losses," Ultrasonics **48**, 85 – 90 (2008).

[47] T. G. Leighton, *The Acoustic Bubble* (Academic Press Limited, 1994).

[48] P. Sridharan, T. L. Jackson, J. Zhang, and S. Balachandar, "Shock interaction with one-dimensional array of particles in air," J. Appl. Phys. **117**, 075902 (2015).